THE JOURNAL OF BIOLOGICAL CHEMISTRY VOL. 291, NO. 31, pp. 16024–16037, July 29, 2016

A Plasma Membrane Association Module in Yeast Amino Acid Transporters*[S]

Received for publication, November 25, 2015, and in revised form, May 18, 2016 Published, JBC Papers in Press, May 19, 2016, DOI 10.1074/jbc.M115.706770

Dušan Popov-Čeleketić[1,2], Frans Bianchi[1], Stephanie J. Ruiz, Febrina Meutiawati, and Bert Poolman[3]

From the Department of Biochemistry, University of Groningen, Groningen Biomolecular Sciences and Biotechnology Institute, and Zernike Institute for Advanced Materials, Nijenborgh 4, 9747 AG Groningen, The Netherlands

Amino acid permeases (AAPs) in the plasma membrane (PM) of *Saccharomyces cerevisiae* are responsible for the uptake of amino acids and involved in regulation of their cellular levels. Here, we report on a strong and complex module for PM association found in the C-terminal tail of AAPs. Using *in silico* analyses and mutational studies we found that the C-terminal sequences of Gap1, Bap2, Hip1, Tat1, Tat2, Mmp1, Sam3, Agp1, and Gnp1 are about 50 residues long, associate with the PM, and have features that discriminate them from the termini of organellar amino acid transporters. We show that this sequence (named PM_{asseq}) contains an amphipathic α-helix and the FWC signature, which is palmitoylated by palmitoyltransferase Pfa4. Variations of PM_{asseq}, found in different AAPs, lead to different mobilities and localization patterns, whereas the disruption of the sequence has an adverse effect on cell viability. We propose that PM_{asseq} modulates the function and localization of AAPs along the PM. PM_{asseq} is one of the most complex protein signals for plasma membrane association across species and can be used as a delivery vehicle for the PM.

Yeast transport amino acids across the plasma membrane (PM),[4] the vacuolar membrane (VM), and to a lesser extent the mitochondrial membrane (1). In the plasma and vacuolar membranes, there are 22 and 11 secondary amino acid transporters, respectively. These transporters are polytopic membrane proteins with 10–14 transmembrane segments. They belong to three superfamilies: amino acid/polyamine/organocation (APC), major facilitator superfamily (MFS), and amino acid/polyamine transporter II (AAPTII) (2). The amino acid transporters belonging to the APC superfamily are often referred to as amino acid permeases (AAPs). They are mainly localized in the PM and can be highly specific, *e.g.* transport only one (enantiomer) amino acid or have a broad range of substrates, like the general amino acid permease Gap1.

Alongside the transporter function, additional roles have been proposed for some AAPs. The most prominent example is Gap1, which has a receptor function whereby it signals the protein kinase A (PKA) pathway (3). This so-called transceptor function has also been described for the phosphate transporter Pho84 and the ammonium transporter Mep2 but not for any other AAPs (4, 5). On the other end of the spectrum is Ssy1, an endoplasmic reticulum (ER)-resident AAP member, that plays a role in amino acid sensing but has no transport function (6–8). The levels of AAPs at the PM are modulated by several transcriptional and post-translational control mechanisms, *e.g.* nitrogen catabolite repression, general amino acid control, and substrate/stress-induced endocytosis (9–12). Although for several AAPs many details of these control mechanisms have been elucidated, quite a few questions concerning the spatiotemporal regulation of AAPs remain unanswered. Which mechanism ensures that the function is performed in the right organelle and what determines the positioning of transporters within different membrane domains are poorly understood (13–15).

Targeting of proteins to a specific organelle occurs through intrinsic signals in their amino acid sequences (16). For instance, the classical nuclear localization signal (cNLS) is a small stretch of basic residues (PKKKRKV) that targets proteins to the nucleus (17, 18). Although targeting signals for several organelles are well defined, information on the targeting of PM-destined proteins is scarce. Upon synthesis in the ER and maturation in the Golgi apparatus, transporters take different vesicular transport routes from the *trans*-Golgi network to the vacuole and to the PM. Those destined for the PM are delivered either directly, through the action of adaptor protein complexes, or can utilize a more specific route, such as the GSE (Gap1 sorting in the endosome) complex in the case of Gap1 (19). Aside from these targeting and localization signals, few proteins throughout species contain specific sequences for association with the PM. These proteins mostly lack transmembrane domains, and their association signals usually have a specific role, mostly in a reversible association with the PM and/or cell signaling. These association signals are often represented by a single predicted amphipathic α-helix but can be more complex (20).

* This work was carried out within the Biotechnology-based Ecologically Balanced Sustainable Industrial Consortium (BE-Basic) Research and Development Program, which was granted a Fonds Economische Structuurversterking subsidy from the Dutch Ministry of Economic Affairs, Agriculture and Innovation (EL&I), and was also supported in part by Netherlands Organisation for Scientific Research (NWO) TOP-GO Program Project 700.10.53. The authors declare that they have no conflicts of interest with the contents of this article.

[S] This article contains supplemental Tables S1–S5 and Figs. S1–S5.

[1] Both authors made complementary and equal contributions to this work.

[2] Supported by European Molecular Biology Organization (EMBO) Long-Term Fellowship EMBO ALTF 1356-2010. Present address: Division of Cell Biology, Dept. of Biology, Faculty of Science, Utrecht University, Padualaan 8, 3584 CH Utrecht, The Netherlands.

[3] To whom correspondence should be addressed. E-mail: b.poolman@rug.nl.

[4] The abbreviations used are: PM, plasma membrane; VM, vacuolar membrane; APC, amino acid/polyamine/organocation; MFS, major facilitator superfamily; AAPTII, amino acid/polyamine transporter II; AAP, amino acid permease; ER, endoplasmic reticulum; NLS, nuclear localization signal; cNLS, classical nuclear localization signal; tcNLS, tandem classical NLS; FRAP, fluorescence recovery after photobleaching; MCC, microcompartment of Can1.

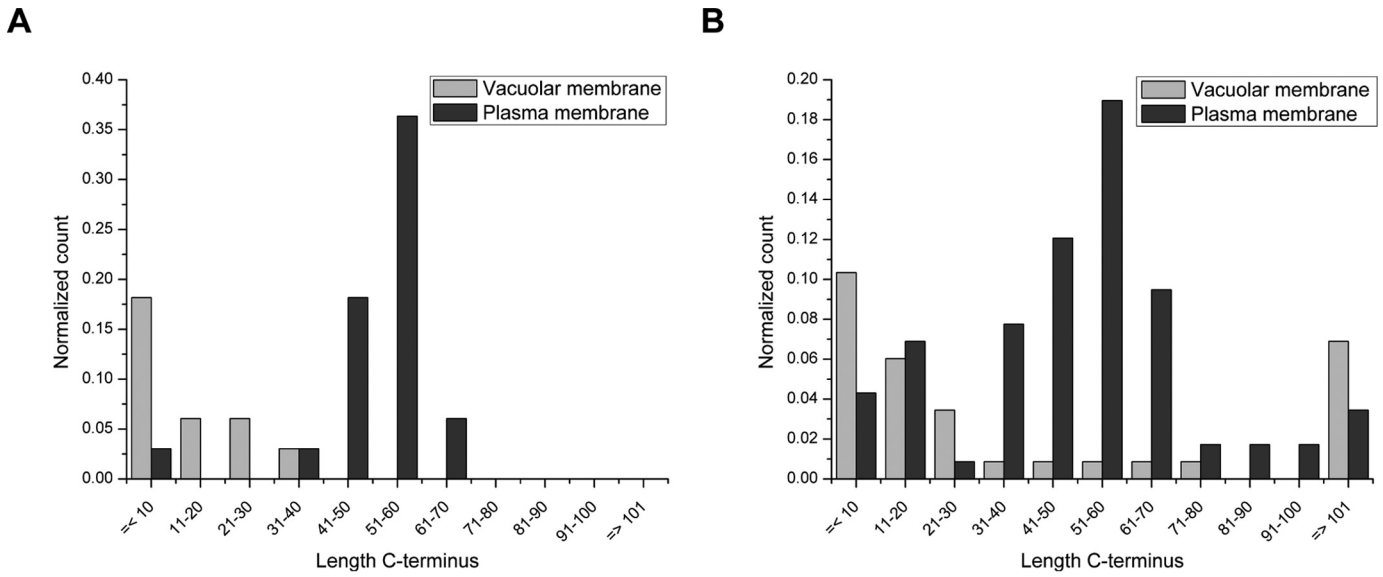

FIGURE 1. **Bioinformatics analysis of *S. cerevisiae* transport proteins.** *A*, amino acid transporters. *B*, secondary transporters in general. C terminus length is defined as the number of amino acid residues following the last predicted transmembrane segment. A list of the proteins analyzed can be found in supplemental Table S1.

Interestingly, several AAPs have distinct localizations within the membrane, most notably Can1 and Tat1, which have been found in a compartment named microcompartment of Can1 (MCC) that co-localizes with a structural scaffold called the eisosome (13, 21). Although amino acid transporters represent a large group of proteins with the same main function, they also have an array of additional roles performed in different locations. It is unclear which cues lead to distinct localizations of these proteins, not only to the designated membrane but also to a distinct location within the PM.

Here, we report on a consensus sequence, PM_{asseq}, found in a subset of AAPs that has a capacity to associate with the yeast plasma membrane. Compared with other sequences mostly found in soluble proteins across species, PM_{asseq}, which is conserved in fungi, is one of the most complex. It consists of two helices, one of them amphipathic, and an FWC signature that allows for its thioesterification with a palmitoyl moiety by palmitoyl acyltransferase Pfa4, thereby creating a lipid tether to the membrane (22). PM_{asseq} interacts with lipids and presumably with proteins in the PM, thereby modulating the position of the transporter in the lipid bilayer. Intriguingly, in reporter constructs containing PM_{asseq} and a strong tandem cNLS, a sequence to target proteins to the nucleus, PM_{asseq} overrides the nuclear localization signal (NLS) in protein targeting. PM_{asseq} can therefore be used as a delivery vehicle for the PM.

Results

C Termini of Amino Acid Transporters in the Plasma Membrane Are Longer than Those of the Vacuolar Membrane—We aimed to identify structural determinants involved in the localization of polytopic membrane proteins either to the PM or VM. All amino acid transporters residing either in the PM or in the VM were grouped on the basis of evolutionary relatedness, that is as members of the APC, MFS, and AAPTII families, and their annotation as amino acid transporters. Sequence alignments of these proteins in *Saccharomyces cerevisiae* failed to identify a motif(s) that could be responsible for protein targeting. We then compared specific segments of individual PM transporters, *i.e.* transmembrane regions, loops, and protein termini, with the corresponding segments of VM transporters. Segments were identified using the membrane topology prediction program TOPCONS (23). This approach revealed significantly longer C termini in PM-resident amino acid transporters than in the corresponding proteins of the VM (Fig. 1*A*). When we extended the comparison to other annotated *S. cerevisiae* transporters, a similar difference in tail length was observed (Fig. 1*B*). In our analysis, we excluded proteins with more than 150 residues in their C termini (four of 79 in PM proteins and eight of 35 VM proteins) as these are known or predicted to form discrete domains with specific functions (supplemental Table S1). Taken together, our analysis *in silico* indicates that there is a correlation between the length of the C terminus and subcellular localization.

Next, we compared the length of the N and C termini of prokaryotic and eukaryotic proteins from the three families (supplemental Fig. S1). In all cases, both the N and C termini are longer in the eukaryotes, which is in agreement with the regulatory roles that these tail regions are known or predicted to have (2). Although the difference in N-terminal length is very distinctive in all families, it is less pronounced for the C termini of the AAPTII and MFS proteins than it is for the APC members.

Zooming in on the localization of the MFS proteins in eukaryotes, we found a wide division of lengths with those with a shorter C terminus annotated to localize mainly to subcellular membranes. Hence, the shift to longer C termini in the APC family could be related to their distinct localization in the PM (supplemental Fig. S2).

Two Types of C Termini in Amino Acid Permeases—The majority of the amino acid transporters localizing to the PM belong to the APC superfamily and are often referred to as

AAPs, a subset belonging to the MFS family (1). An alignment of the C termini of AAP sequences (see "Experimental Procedures") showed conserved clusters of aromatic residues at the beginning and at the end of the sequences together with alternating positively and negatively charged clusters (Fig. 2*A*). Nine transporters contain the FWC signature at the very end, and one transporter (Mmp1) contains the related FFC sequence (24). The FWC-containing C termini have been reported to contain a conserved α-helix (25). Our secondary structure analysis identified a second predicted α-helix at the very end of the sequence that is conserved in all but two of the AAPs, Dip5 and Agp2 (Fig. 2*A*). We refer to the upstream and downstream helices as Ha and Hb, respectively. Helical wheel projections and the calculated hydrophobic moment show that Hb has features similar to amphipathic motifs known to bind membranes, including clusters of positive and/or aromatic residues (20) (Fig. 2*B*). The C terminus of Uga4, a non-core member of the AAPs that resides in the vacuolar membrane and was used as a control in this study, is predicted to have a single non-amphipathic α-helix without aromatic clusters (Fig. 2, *A* and *B*).

The predicted secondary structure was verified by circular dichroism (CD) using a synthetic peptide corresponding to the last 31 residues of Gap1 (Fig. 2*C*). The CD spectrum showed a clear positive peak at 193 nm and negative peaks at 208 and 222 nm that are characteristic of α-helical polypeptides (26). This signal became even more pronounced in the presence of trifluoroethanol (27), thus confirming the predictions *in silico*.

We determined the physiological relevance of the C-terminal tail of AAP transporters by generating a series of *S. cerevisiae* strains containing AAPs in which the last 10 amino acid residues were deleted and thus most of the amphipathic helix Hb. Wild-type (WT) and truncated versions of the transporters were tagged with the fluorescent protein mKate2, and the fusions were expressed from the endogenous promoters on the chromosome. No significant differences in expression or localization between WT and truncated mKate2 transporters were visible by confocal microscopy, probably due to the relatively low expression levels (supplemental Fig. S3). Low expression levels could be the consequence of the added tag on the C terminus. Irrespective of this, strains expressing truncated versions of a subset of AAPs exhibited a distinct phenotype under restricted growth conditions. The Hb helix in AAPs with the FWC signature is required for growth on a non-fermentable carbon source (glycerol; SG) as shown for Gap1 and Tat2 (Fig. 2*D*). In contrast, removal of the last 10 residues of Lyp1 and Can1, AAPs responsible for the transport of lysine and arginine, respectively, did not have a strong adverse effect on cell growth. Although in the case of Lyp1Δ10 colonies were smaller, the strain was viable. Contrary to deleting the Hb helix, deletion of the entire gene for Gap1 did not affect growth on SG, indicating that the C termini of Gap1 and possibly Tat2 control a negative-dominant function of the protein. The strains expressing truncated versions of AAPs exhibited no visible growth defect when grown on a fermentable carbon source (glucose; SD). Thus, on the basis of physiological studies, the C termini fall in two categories: those with the FWC motif seem more important for cell growth under restrictive conditions than those without this signature motif.

C Termini of Amino Acid Permeases Associate with the Plasma Membrane—As amphipathic helices in many proteins have a tendency to interact with membranes, we asked whether the C-terminal segments of the AAPs alone associate with the PM or other membranes in the cell. This has previously been shown for a region of the C terminus of Bap2 (28). The C-terminal segments of selected AAPs (sequences depicted in Fig. 2*A*), were fused to GFP, and the genes were placed under the control of an inducible promoter and expressed in *S. cerevisiae*. Two clear localization patterns were observed. C termini containing the FWC signature mainly localized to the cell periphery (Fig. 3*A*), whereas those without the FWC signature were soluble and/or partially aggregated in the cytosol (Fig. 3*B*). This suggests that the FWC signature may play a role in the association of the C termini of AAPs with the PM. To confirm this suggestion, we added the FWC tripeptide sequence to the cytosolically localized C termini. In the case of Alp1, Lyp1, and Can1, the addition of FWC caused the reporter protein to associate with cell membranes (Fig. 3*C*). The relevance of the AAP C-terminal sequence upstream of FWC for association with the membrane is demonstrated by the C terminus of Uga4, which failed to localize at the cell periphery with or without the addition of the FWC signature.

Interestingly, in contrast to the homogenous distribution at the PM of most FWC-containing reporters, the C terminus of the histidine transporter Hip1 led to a patchy distribution of the protein in the cell. A similar pattern, but to a lesser extent, was observed for Can1C+FWC and Alp1C+FWC. Heterologous expression of the reporters in *Pichia pastoris* displayed the same distribution pattern (supplemental Fig. S4A). The phenotypic conservation in *P. pastoris* is in agreement with the conservation of the AAP C termini, including the FWC motif and the upstream basic and aromatic residues, in other budding yeast (supplemental Fig. S4C and supplemental Table S2).

The Membrane Association Signal of AAPs Is Multipartite—To investigate which residues are important for membrane association, we analyzed the C-terminal sequences in more detail by deleting clusters of three to five conserved residues from the Gap1C reporter protein (Fig. 4, *A* and *B*). Deletion of WKLF, DID, RRE, and DLD did not affect the association of the GFP-tagged C terminus with the PM. Deletions of EEK (in the middle of helix Ha), PRWYR (half of helix Hb), and FWC led to a cytosolic localization with sporadic aggregate formation. CD analysis of synthetic peptides corresponding to these deletions showed a reduced α-helical signature compared with wild-type Gap1C (Fig. 4*C*). For the ΔPRWYR and ΔFWC peptides, the spectra are shifted toward that expected for a disordered protein, namely a negative peak at around 195 nm and very little ellipticity above 210 nm (26) This suggests that the α-helical secondary structure of Gap1C is necessary for its association with the plasma membrane.

Sequences capable of forming amphipathic helices and suggested to associate with the PM have been identified in a number of proteins throughout species (20). The most investigated sequence in yeast, which at the same time represents a rather complex association signal, is that of Ist2, the cortical ER protein involved in ER-PM tethering (8, 29). The association of Ist2 with the PM requires one amphipathic helix followed by a clus-

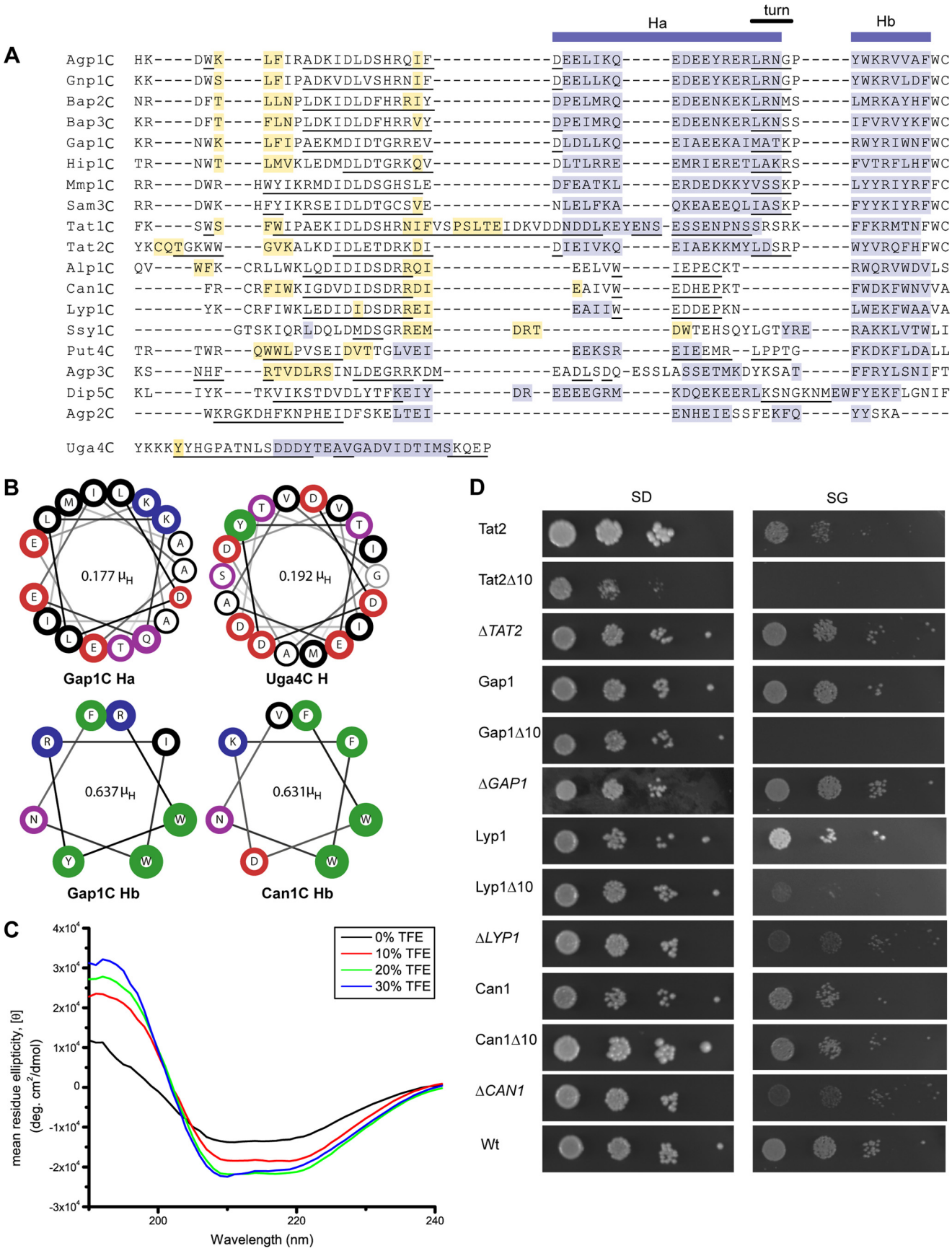
A
Ha
turn
Hb
Agp1C HK----DWK----LFIRADKIDLDSHRQIF----------DEELIKQ-----EDEEYRERLRNGP-----YWKRVVAFWC
Gnp1C KK----DWS----LFIPADKVDLVSHRNIF----------DEELLKQ-----EDEEYKERLRNGP-----YWKRVLDFWC
Bap2C NR----DFT----LLNPLDKIDLDFHRRIY----------DPELMRQ-----EDEENKEKLRNMS-----LMRKAYHFWC
Bap3C KR----DFT----FLNPLDKIDLDFHRRVY----------DPEIMRQ-----EDEENKERLKNSS-----IFVRVYKFWC
Gap1C KR----NWK----LFIPAEKMDIDTGRREV----------DLDLLKQ-----EIAEEKAIMATKP-----RWYRIWNFWC
Hip1C TR----NWT----LMVKLEDMDLDTGRKQV----------DLTLRRE-----EMRIERETLAKRS-----FVTRFLHFWC
Mmp1C RR----DWR---HWYIKRMDIDLDSGHSLE----------DFEATKL-----ERDEDKKYVSSKP-----LYYRIYRFFC
Sam3C RR----DWK---HFYIKRSEIDLDTGCSVE----------NLELFKA-----QKEAEEQLIASKP-----FYYKIYRFWC
Tat1C FK----SWS----FWIPAEKIDLDSHRNIFVSPSLTEIDKVDDNDDLKEYENS-ESSENPNSSRSRK-----FFKRMTNFWC
Tat2C YKCQTGKWW----GVKALKDIDLETDRKDI----------DIEIVKQ-----EIAEKKMYLDSRP-----WYVRQFHFWC
Alp1C QV----WFK--CRLLWKLQDIDIDSDRRQI----------EELVW-----IEPECKT----------RWQRVWDVLS
Can1C -------FR--CRFIWKIGDVDIDSDRRDI----------EAIVW-----EDHEPKT----------FWDKFWNVVA
Lyp1C -------YK--CRFIWKLEDIDIDSDRREI----------EAIIW-----EDDEPKN----------LWEKFWAAVA
Ssy1C ----------GTSKIQRLDQLDMDSGRREM--------DRT----------DWTEHSQYLGTYRE----RAKKLVTWLI
Put4C TR----TWR---QWWLPVSEIDVTTGLVEI----------EEKSR-----EIEEMR--LPPTG-----FKDKFLDALL
Agp3C KS----NHF----RTVDLRSINLDEGRRKDM----------EADLSDQ-ESSLASSETMKDYKSAT-----FFRYLSNIFT
Dip5C KL----IYK---TKVIKSTDVDLYTFKEIY--------DR--EEEEGRM-----KDQEKEERLKSNGKNMEWFYEKFLGNIF
Agp2C -------WKRGKDHFKNPHEIDFSKELTEI----------ENHEIESSFEKFQ-----YYSKA-----
Uga4C YKKKYYHGPATNLSDDDYTEAVGADVIDTIMSKQEP
B
0.177 μH
Gap1C Ha
0.192 μH
Uga4C H
0.637 μH
Gap1C Hb
0.631 μH
Can1C Hb
C
0% TFE
10% TFE
20% TFE
30% TFE
mean residue ellipticity, [θ] (deg. cm²/dmol)
4x10⁴
3x10⁴
2x10⁴
1x10⁴
0
-1x10⁴
-2x10⁴
-3x10⁴
200
220
240
Wavelength (nm)
D
SD
SG
Tat2
Tat2Δ10
ΔTAT2
Gap1
Gap1Δ10
ΔGAP1
Lyp1
Lyp1Δ10
ΔLYP1
Can1
Can1Δ10
ΔCAN1
Wt

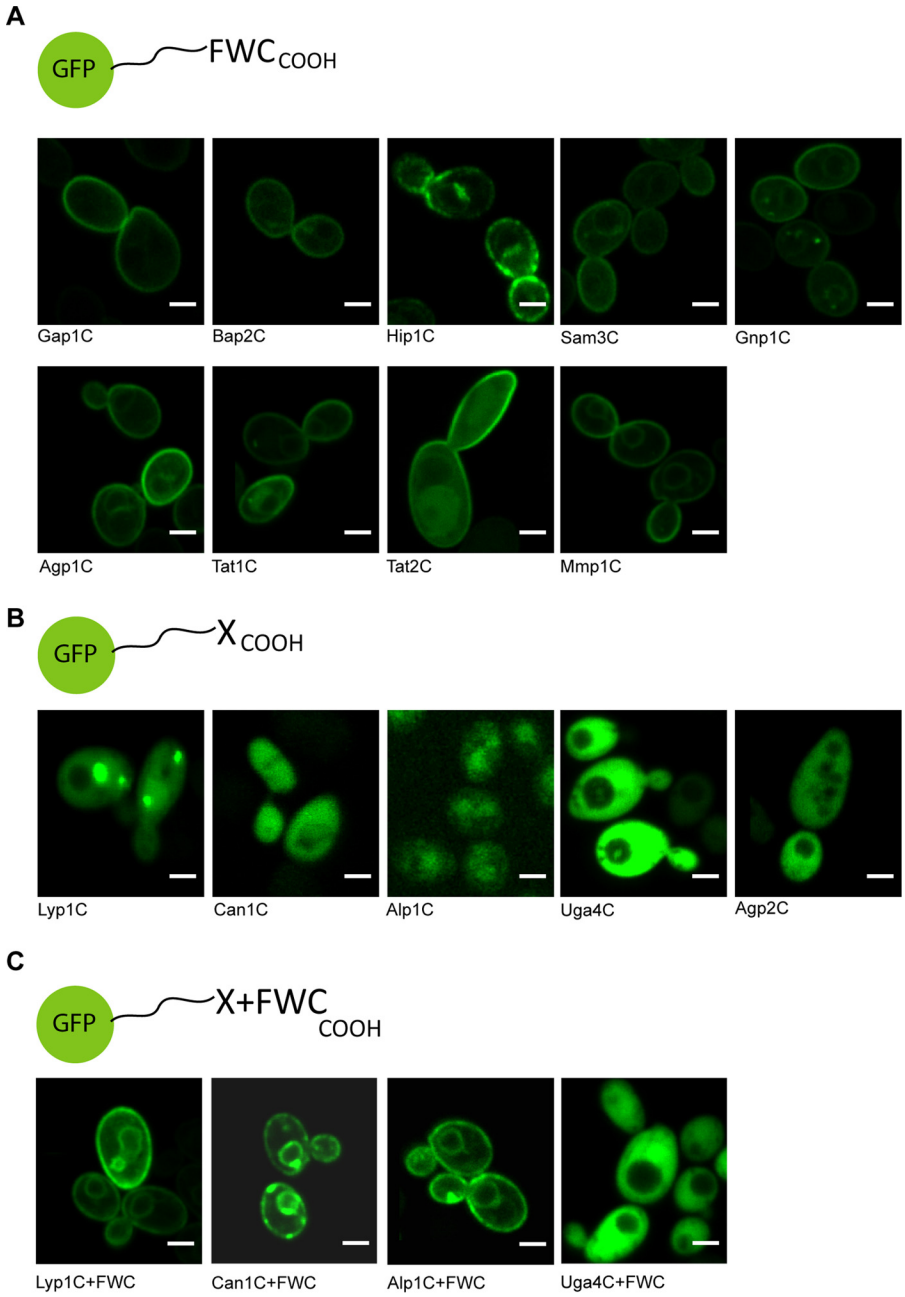

FIGURE 3. **Localization of GFP-fused C-terminal reporters.** *A*, C-terminal reporters with the FWC motif localize to the cell periphery. *B*, C-terminal reporters without the FWC motif localize to the cytoplasm. *C*, the addition of FWC to the C terminus of Alp1, Lyp1, and Can1, but not Uga4, results in membrane association. *Scale bars,* 2 μm.

ter of positively charged residues in the C terminus (30). In contrast to the C terminus of AAPs, the amphipathic C terminus of Ist2 fused to GFP led to a minor association with the PM, and the vast majority of the protein remained soluble in the cytosol in agreement with previous studies (31) (Fig. 4*D*).

In other amphipathic helices that associate with cellular membranes, *e.g.* Mid1 from *Schizosaccharomyces pombe* or Ste5 from *S. cerevisiae*, an NLS or an NLS-like sequence was found within or in close proximity of the helix, which under certain conditions localized the proteins to the nucleus (32, 33).

FIGURE 2. **C termini of amino acid transporters contain a functional amphipathic α-helix.** *A*, multiple sequence alignment of C termini from core members of the AAP family showing predicted secondary structure features. *Orange shading*, β-sheet; *purple shading*, α-helix; *underlined*, β-turns. *B*, helical wheel projections of C-terminal α-helices from Gap1, Can1, and Uga4. Amino acid properties are indicated by *line thickness* (side chain size) and color (*black*, hydrophobic/aliphatic; *green*, aromatic; *blue*, positive; *red*, negative; *purple*, hydrophilic). The hydrophobic moment (μ_H) value determined by the method of Eisenberg *et al.* (64) is shown in the *center* of the helix. *C*, far-UV CD spectra of a synthetic peptide corresponding to the last 31 residues of Gap1. The addition of trifluoroethanol (*TFE*) enhances the α-helical signature. *D*, growth of strains expressing full-length or C-terminally truncated amino acid permeases. All are expressed with a C-terminal mKate2 tag from their endogenous promoter on the chromosome. 10-fold serial dilutions of cells were spotted onto SD and SG plates and grown for 3–4 days at 30 °C. *deg*, degrees.

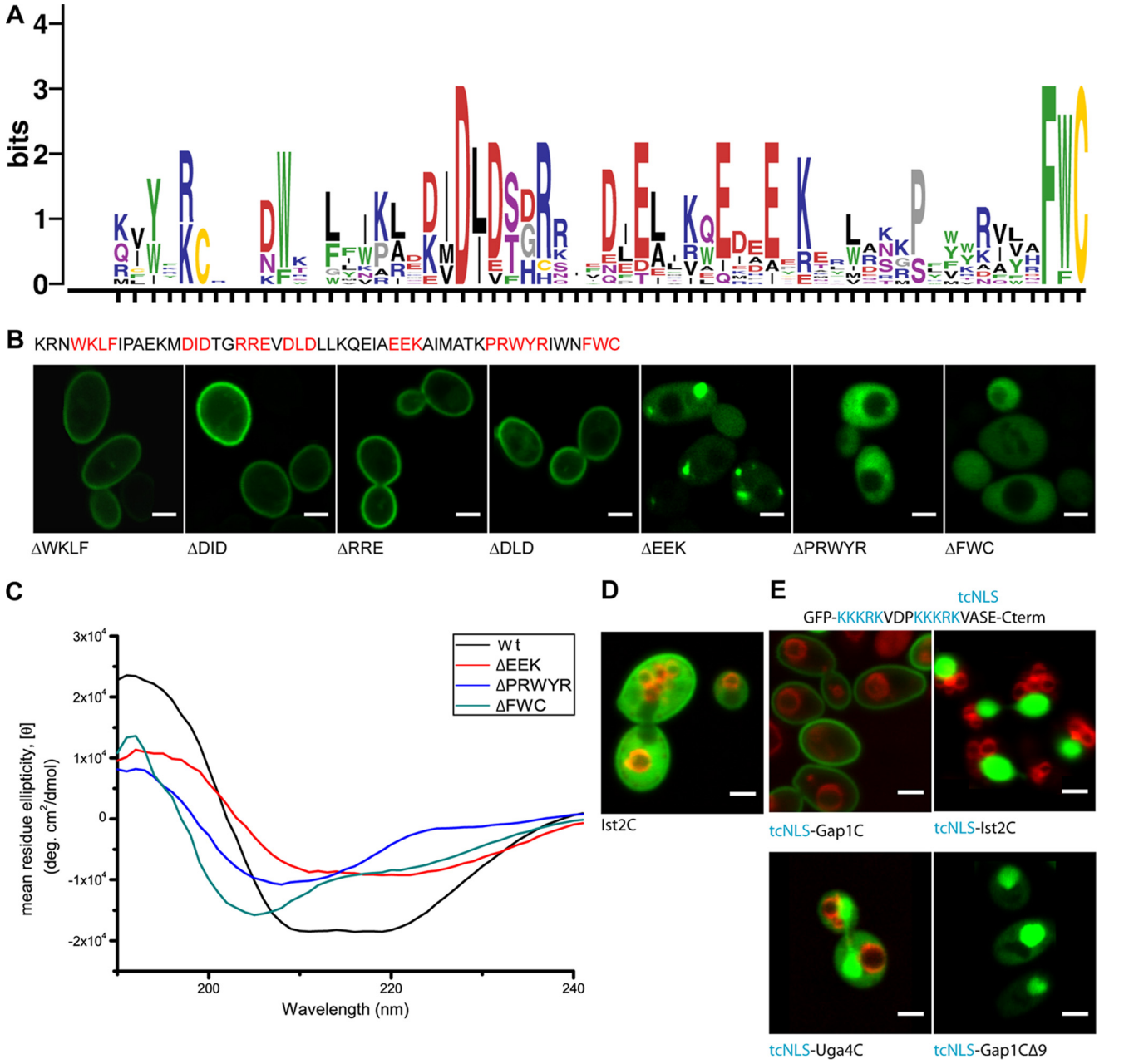

FIGURE 4. **FWC motif and upstream amphipathic helix are required for association at the cell periphery, and the targeting signal is stronger than a tcNLS.** *A*, sequence logo of C-terminal sequences that are able to localize GFP to the cell periphery. The image was prepared using WebLogo (66) and colored according to amino acid properties (*black*, hydrophobic/aliphatic; *green*, aromatic; *blue*, positive; *red*, negative; *purple*, hydrophilic; *gray*, conformationally special; *orange*, cysteine). *B*, deletions within the Gap1 C terminus show that the FWC motif and two upstream sequences within the predicted α-helices are crucial for localization to the cell periphery. *C*, far-UV CD spectra of synthetic peptides corresponding to the last 31 residues of the Gap1 C terminus as well as the truncated versions ΔEEK, ΔPRWYR, and ΔFWC. All samples contained 10% 2,2,2-trifluoroethanol. *D*, C terminus of Ist2 fused to GFP (*green*). Staining of the vacuolar membrane with FM4-64 is shown in *red*. *E*, C termini of Gap1, Ist2, and Uga4 with GFP-tcNLS fused N-terminally of the C terminus (*green*). Staining of the vacuolar membrane with FM4-64 is shown in *red*. *Scale bars*, 2 μm. *deg*, degrees.

We therefore tested the effect of the addition of a very strong tandem classical NLS (tcNLS) derived from Heh2 (34) to the C-terminal sequences of the AAP proteins. The addition of the tcNLS upstream of the C terminus of Gap1C did not affect its association with the PM (Fig. 4*E*). Conversely, addition of the NLS to the GFP-tagged C terminus of Ist2 localized the reporter to the nucleus. The same observation was made for GFP-Uga4C, GFP alone, and Gap1C lacking most of the amphipathic sequence, demonstrating that the membrane association signal found in AAPs is relatively strong when compared with those for targeting to organellar membranes. In conclusion, the sequence responsible for PM association (hereafter referred to as PM_{asseq}) of the C termini of yeast AAPs is composed of two α-helices with the downstream helix being amphipathic and an FWC signature at the very C termini of the proteins.

A Palmitoyl Moiety Anchors the C Termini of AAPs to the PM—The conserved FWC sequence within yeast AAPs was previously identified in a large scale analysis *in silico*, and it was shown for a subset of AAPs that the C-terminal cysteine residue serves as a palmitoylation site (22, 24). Palmitoylation is a

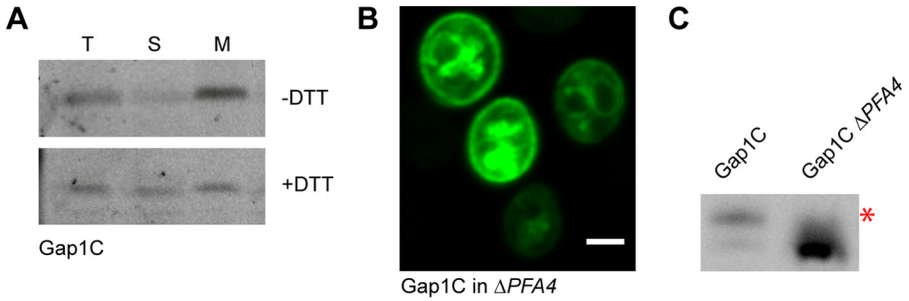

FIGURE 5. **Palmitoylation of Gap1C is Pfa4-mediated but is not essential for association with membranes.** *A*, in-gel fluorescence imaging. Total (*T*), soluble (*S*), and membrane (*M*) fractions isolated from cells expressing GFP-Gap1C were preincubated with (+) and without (−) DTT and then separated by 15% SDS-PAGE. The membrane fraction shows enrichment of Gap1C in the absence of DTT. *B*, Gap1C in Δ*PFA4* associates with the PM and internal membranes. *Scale bar*, 2 μm. *C*, a molecular weight shift is observed for GFP-Gap1C by in-gel fluorescence of whole cell extracts from wild-type and Δ*PFA4* yeast cells separated by 21% SDS-PAGE. The palmitoylated form of Gap1C is indicated with a *red asterisk*.

reversible post-translational modification that is sensitive to reducing conditions (2, 35). To examine whether the C termini derived from AAPs are indeed palmitoylated, we analyzed GFP-Gap1C from yeast cells, incubated in the presence or absence of DTT, using 15% SDS-PAGE. The amount of Gap1C in the membrane fraction was significantly lower after DTT incubation, indicating that the reporter protein was palmitoylated (Fig. 5*A*).

To identify the enzyme responsible for the palmitoylation of GFP-Gap1C, we transformed yeast strains lacking one of the seven palmitoyl acyltransferases. Only in the strain lacking Pfa4 was an effect seen with most of the reporter protein relocalizing to the cytosol and the internal membranes (Fig. 5*B*). In the strains lacking any of the other six palmitoyl acyltransferases, localization of GFP-Gap1C was the same as in the wild-type background (supplemental Fig. S5). This is in line with the previous observation that the palmitoylation of full-length AAPs is Pfa4-dependent (22). It also demonstrates that the C-terminal sequence of Gap1 is sufficient for recognition and palmitoylation by Pfa4 despite not being part of a polytopic membrane protein.

In the strain lacking Pfa4, the Gap1C reporter protein remained partially associated with internal membranes. This is consistent with the fact that reducing conditions did not completely remove GFP-Gap1C from the membrane fraction (Fig. 5*A*). The clear difference in PM association between Gap1C in the Δ*PFA4* genetic background and Gap1C lacking the FWC tripeptide (compare Figs. 5*B* and 4*B*) is explained by the fact that in the former case the reporter protein lacks the palmitoyl moiety, whereas in the latter case it lacks not only the palmitoyl moiety but also functional helix Hb (see Fig. 4*C*).

It is, however, possible that another palmitoyl acyltransferase is able to palmitoylate Gap1C in the absence of Pfa4, thereby contributing to the association of the reporter protein with the lipid bilayer. To exclude this, we compared lysates isolated from cells expressing GFP-Gap1C in the wild-type and Δ*PFA4* genetic backgrounds. We analyzed these lysates by high percentage SDS-PAGE, which allowed us to discriminate the lack of a 0.25-kDa palmitoyl moiety (Fig. 5*C*). The experiment confirmed that Pfa4 is solely responsible for the palmitoylation of Gap1C. Thus, the residual membrane association in the Δ*PFA4* strain is due to properties of the upstream amino acid sequence, more specifically the presence of the intact Hb helix.

Variations in the C-terminal Sequences of AAPs Are Reflected in Different Localization Patterns at the PM—Localization differences relating to the amino acid sequence, separate from palmitoyl-dependent mechanisms, were also seen for other C termini. When expressed in the Δ*PFA4* genetic background, GFP-Bap2C is completely cytosolic, whereas Hip1C retains its distinct patchy distribution, and Alp1C+FWC remains at the cell periphery (Fig. 6*A*). The same patterns were seen for Bap2C and Hip1C with the C-terminal cysteine changed to serine, a mutation that has been shown to fully abolish palmitoylation in full-length AAPs (22). The presence or absence of palmitoyl modifications under these conditions was confirmed by analyzing protein extracts by high percentage SDS-PAGE (Fig. 6*B*). Analysis of the localization patterns for the rest of the transporters in the Δ*PFA4* genetic background showed that Tat2C, Gnp1C, and Sam3C were completely cytosolic, whereas a fraction of Mmp1C, Tat1C, and Lyp1+FWC remained associated with the membrane (Fig. 6*C*). In contrast, lack of the palmitoyl moiety in Can1C+FWC and Alp1C+FWC led to an almost exclusive localization to distinct spots at the periphery of the cell. Expression of reporter constructs in *P. pastoris* showed the same localization for $Bap2C_{FWS}$ and $Hip1C_{FWS}$, indicating conservation of palmitoylation and protein partner binding (supplemental Fig. S4B).

The C-terminal Sequences of AAPs Have Different Mobility at the PM—The mobility of the reporters at the cell periphery was measured by fluorescence recovery after photobleaching (FRAP). From the fluorescence recovery, we determined the lateral diffusion coefficient and the mobile fraction. With the exception of Hip1C, fluorescence recovery of C termini was relatively fast in comparison with integral membrane proteins as shown by comparing Gap1C and Pma1 (Fig. 7*A*). The diffusion coefficient of the palmitoylated reporters is approximately 2 orders of magnitude higher than that of the full-length integral membrane proteins (Fig. 7*B*). When Gap1C, Tat1C, and Mmp1C were expressed in the Δ*PFA4* strain, the reporters localized to the cytoplasm and the diffusion coefficients were 1 order of magnitude higher than those of the palmitoylated reporters (Fig. 7*B*).

The FRAP experiments showed no recovery of Hip1C (Fig. 7, *A* and *C*). The static nature of Hip1C is consistent with its patchy distribution at the PM and suggests interaction with a static partner at the periphery of the cell. Less than 50% recov-

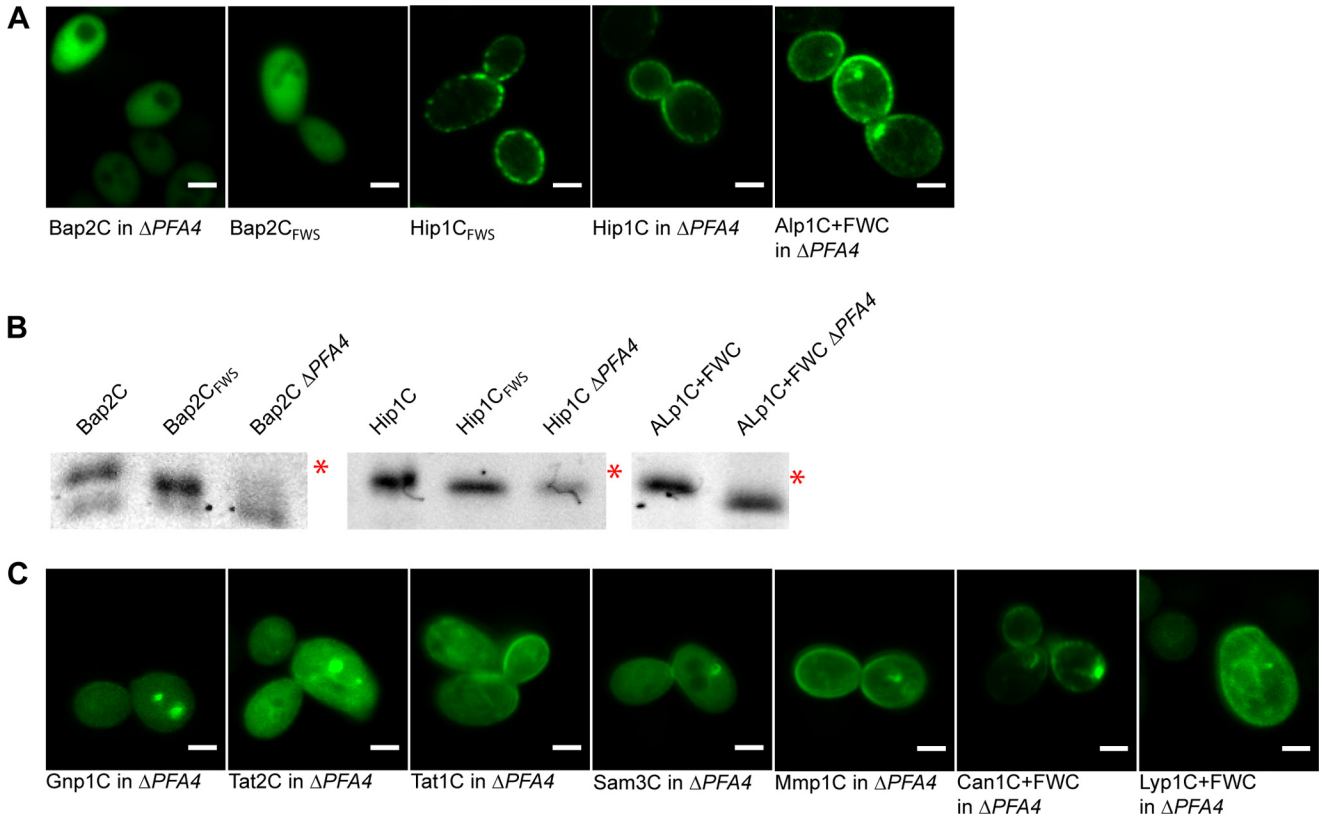

FIGURE 6. **The absence of palmitoylation shows discriminative phenotypes for C termini.** *A*, in the absence of a palmitoyl moiety, some C-terminal sequences are still able to direct GFP to the cell periphery (Hip1C and Alp1C), whereas GFP-Bap2C is located in the cytoplasm. *B*, in-gel fluorescence imaging of whole cell extracts separated by SDS-PAGE. For GFP-Bap2C, -Hip1C, and -Alp1C, fluorescent bands are seen at two positions. The higher band (indicated with a *red asterisk*) is the modified form, running slower due to the palmitoyl moiety. *C*, in cells lacking Pfa4, three phenotypes are observed for GFP N-terminally fused to C termini: cytoplasmic localization (Gnp1C and Tat2C), enrichment at the membranes (Tat1C, Sam3C, Mmp1C, and Lyp1C+FWC), and distinct localizations at the periphery of the cell (Can1C+FWC). *Scale bars*, 2 μm.

ery was observed for Can1C+FWC and Alp1C+FWC (Fig. 7*C*). Expression of Can1C+FWC and Alp1C+FWC in the Δ*PFA4* genetic background reduced the recovery even further (Fig. 7*D*). The lack of mobility and distinct localization of some proteins at the periphery of the cell suggests either (i) the presence of static protein-binding partners, (ii) slow on/off rates of association, or (iii) mobility at a time scale similar to that of polytopic membrane proteins.

Discussion

Throughout species, a number of proteins contain sequences that are capable of associating with membranes. These sequences can serve as signals for targeting to a specific organelle but can also represent a critical factor for a protein to perform its function at the designated site. Often these sequences contain an amphipathic α-helix, which has the ability to associate with the membrane, *e.g.* as shown for Ist2 and Ssy1 in *S cerevisiae* (8, 29). Here, we report on a membrane association module comprising a palmitoylated sequence (PM_{asseq}) present in the C terminus of 10 yeast AAPs. It consists of two helices, one amphipathic, and an FWC signature sequence at the very end with a Cys-linked palmitoyl moiety. This is a highly complex and unique membrane association signal identified for polytopic PM proteins, and we propose that it plays a role in the localization and function of AAPs within membrane microdomains through its association with specific proteins and/or lipids.

In our combined sequence/topology analysis of secondary transporters, we noticed that the C termini of PM-resident proteins are on average longer than those of VM-resident proteins. The observed division is especially pronounced among secondary amino acid transporters. Residues from the C termini of several AAPs have been assigned roles in PM targeting and regulation of function. The KPRWYR motif in the C terminus of Gap1 has been shown to be important for trafficking from the trans-Golgi network to the PM (19). In addition, a dileucine motif in a predicted α-helical region of the Gap1 C terminus is required for NH_4^+-induced endocytosis (25, 36). Deletion of the last 28 residues of Bap2 was shown to stabilize the protein at the plasma membrane by decreasing its basal turnover (28). It is not known whether these functions of the C-terminal motifs are conserved among AAPs. In contrast, a diacidic motif shortly after the last transmembrane region, (M/I/V)D(L/I/V)D, is required for many transporters in coat protein complex II vesicle packing and is therefore conserved among all AAPs (37, 38).

We report on a sequence, PM_{asseq}, present in 10 FWC-containing AAPs and partially conserved in the other members of the AAP family that has a capacity to associate with the PM. Sequence comparisons indicate that PM_{asseq} is widely conserved among budding yeast (supplemental Fig. S4C). It has two predicted α-helices with the downstream helix being amphipathic, which we confirmed for Gap1 by CD spectroscopy. Similar to sequences found in a number of soluble pro-

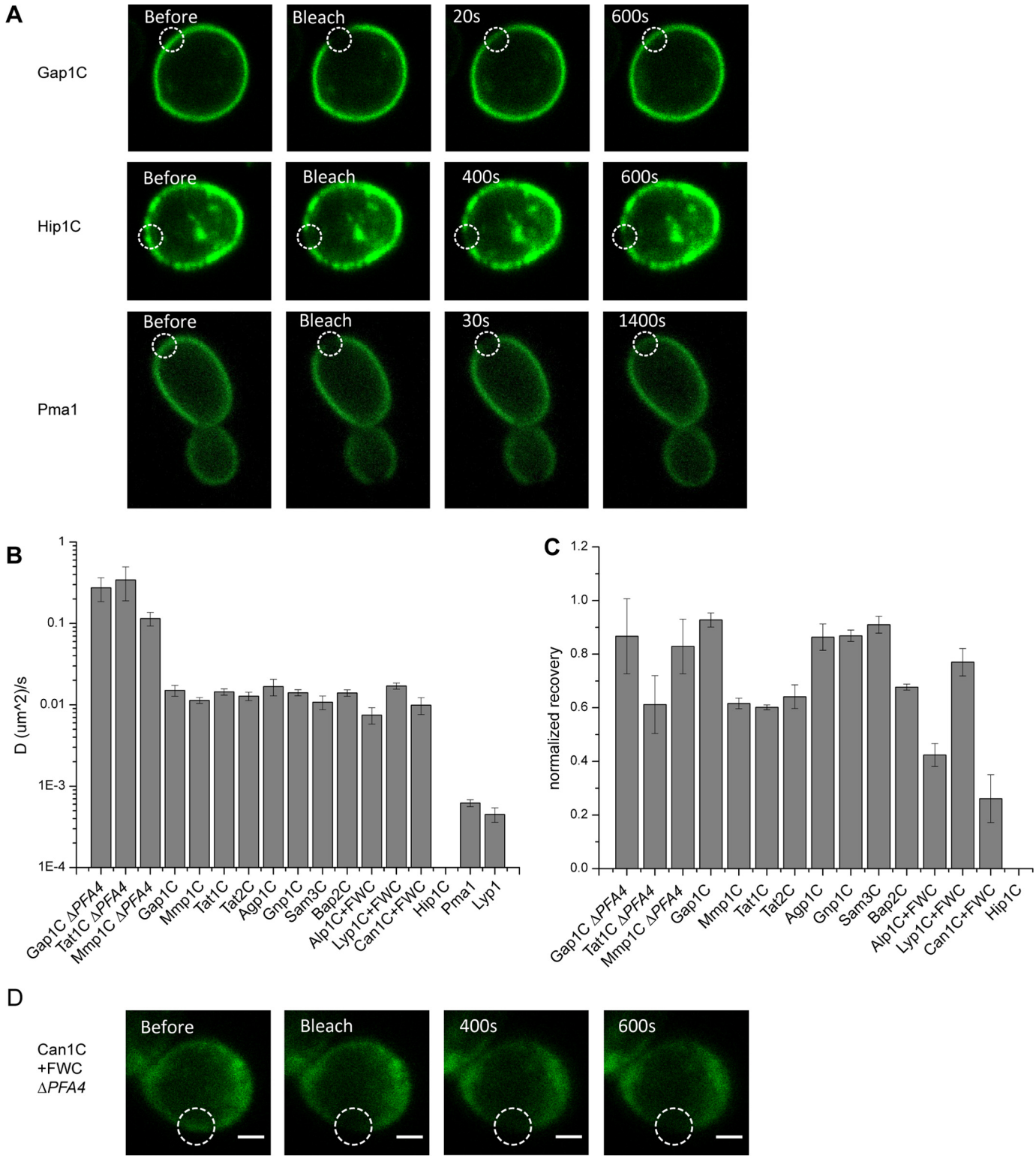

FIGURE 7. **High variation in mobility suggests sequence-specific interactions.** Diffusion coefficients for lateral diffusion along the cell periphery were determined using FRAP. Full-length Lyp1 and Pma1, the plasma membrane proton ATPase, were included for comparison. *A*, confocal microscopy images demonstrating the recovery after photobleaching for immobile (GFP-Hip1C) and mobile (GFP-Gap1C, Pma1) constructs. Diffusion coefficients (*B*) and normalized recovery (*C*) were calculated from exponential recovery profiles. Mobile fraction *error bars* represent the standard deviation between the measurements. *D*, confocal microscopy images demonstrating the recovery after photobleaching for GFP-Can1C+FWC in Δ*PFA4*. *Scale bars*, 1 μm.

teins, these sequences associate with the membrane (20). Membrane association signals are frequently found in proteins that bind to specific lipids and often comprise amphipathic α-helical structures associating with the membrane. One notable example is the membrane association signal found in the N-terminal 18 residues of Huntingtin. It forms an amphipathic α-helical membrane-binding domain that can reversibly target to vesicles and the ER (39). ER and vesicular membrane associ-

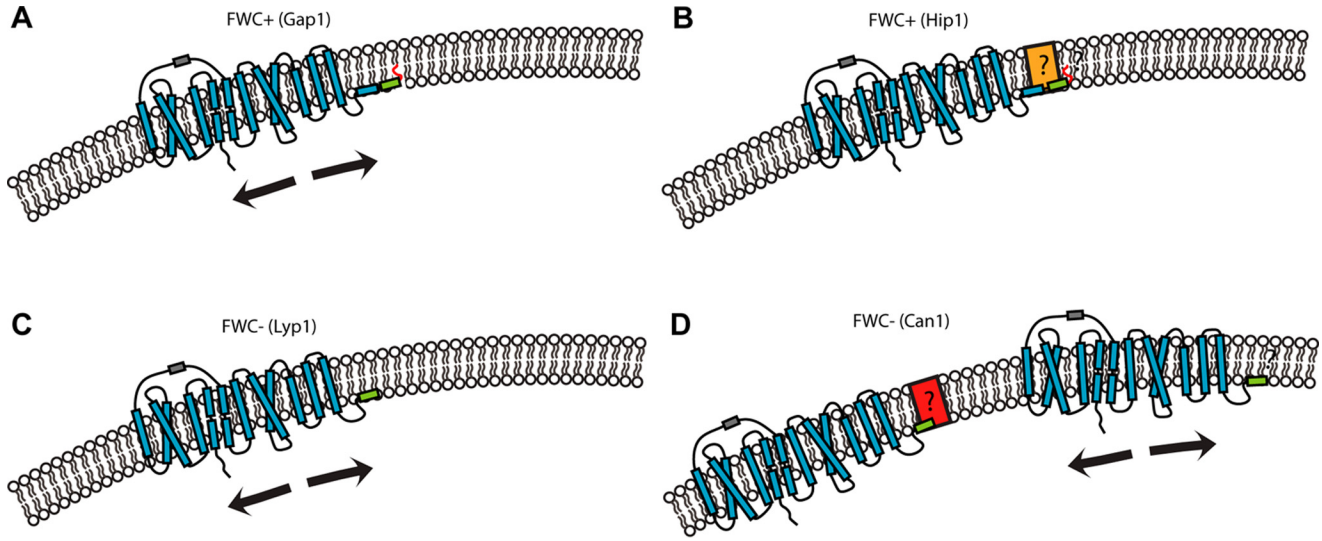

FIGURE 8. **Model describing the association with the PM of C termini of different AAPs.** *A*, proteins with FWC-containing C termini have a strong association with specific lipids in the PM with a possible regulatory role for signaling functions. *B*, Hip1 most likely interacts with a static binding partner. This interaction is directed by the sequence upstream of the FWC signature and it is not dependent on the presence of the palmitoyl moiety. *C*, the C terminus of proteins lacking the FWC signature, like Lyp1, may have weak lipid binding affinity, enabling lateral probing of the membrane surface. *D*, proteins without FWC-containing C termini in which the C termini have transient interactions with integral membrane proteins as in the case of Can1 and Alp1.

ation signals present in fungal proteins are found in transcription factors and proteins involved in vesicular transport and in cell division (32, 40, 41). In *S. cerevisiae*, membrane association signals for targeting to the PM are found in proteins of signal transduction pathways (42, 43). Plasma membrane association signals are not common in PM-residing integral membrane proteins, and they do not serve as primary targeting signals as delivery to the PM is via vesicular transport. The role of such signals is usually connected with a specific function of the protein as is the case for the LRRLL motif in EGF receptor of mammalian cells (44).

The membrane association signal described here is unique as it is present in polytopic PM proteins. Its unusual strength is explained by its multipartite nature as membrane association is enabled through the interactions of not one but two helices and a palmitoyl moiety attached to the C-terminal cysteine. Helix Hb of PM_{asseq} is highly conserved, strongly amphipathic in nature, and present in AAPs that do not contain the FWC signature; *i.e.* these proteins are not palmitoylated. The importance of this sequence is demonstrated by the finding that the C-terminal sequence of AAPs without FWC can associate with the PM upon the addition of FWC to the C terminus. Importantly, in these proteins, the upstream helix Ha is either missing or predicted to be significantly shorter than that in AAPs with FWC. We also demonstrated that the C terminus is essential for palmitoylation by Pfa4. Palmitoylation of these sequences increases the specificity of targeting to the plasma membrane but is not strictly required for membrane association.

The complex and redundant nature of PM_{asseq} may relate to its capacity to interact with different partners in the membrane. The PM_{asseq}s of different AAPs neither display uniform localization nor do they lead to a similar mobility of the proteins along the membrane surface. In the case of Hip1, Alp1, and Can1, the association signal modulates the localization of the transporter along the plasma membrane as is visible by the formation of distinct patches of protein. The correlation between patchy localization and slow diffusion indicates possible partners in the PM that may interact in a highly specific manner with a subset of AAPs. FRAP analyses suggest that in the case of Hip1C the protein partner is fully static, and there is no exchange after initial binding. For Alp1C and Can1C, distinct mobile and immobile fractions are observed. Upon removal of the palmitoylation site, there is no recovery, suggesting a static partner.

For Gap1 and Tat2, removal of the last 10 amino acids leads to diminished growth on a non-fermentable carbon source, whereas the expression and gross PM localization are not affected. A specific role for the C terminus of Gap1 in nutrient sensing has been proposed before as truncated versions of the Gap1 show an increased PKA signaling phenotype (3). Constitutive PKA signaling is reported to inhibit growth on any carbon source other than glucose (45). Interestingly, deletion of the gene coding for Gap1 showed no adverse effect on growth, suggesting a negative-dominant interaction of the C terminus with other parts of the protein. Amphipathic α-helices have been shown to play roles in autoinhibition mechanisms with the most well studied example being CTP:phosphocholine cytidylyltransferase (46).

Taking into account different motilities, different localization patterns, and redundancy for PM association, we put forward the following model (Fig. 8). Upon vesicular delivery of AAP to the PM, the C terminus associates with the lipids on the cytosolic side of the PM through its two helices and the palmitoyl tail. The complete association signal found in FWC-containing proteins is necessary for strong association with specific lipid(s)/domains in the PM that modulate the function of the transporters. Gap1 is one example of this group of proteins (Fig. 8*A*). Hip1 most likely interacts with a static binding partner, enabling the transporter to perform its function at a specific location in the PM (Fig. 8*B*). This interaction is directed by the sequence upstream of the FWC signature, and it is not dependent on the presence of the palmitoyl moiety. This unique local-

ization pattern is interesting in light of the finding that Hip1 is the only AAP whose gene could not be deleted in a large scale genetic screen (47). The C terminus of proteins lacking the FWC signature, such as Lyp1, may have weak lipid binding affinity as evidenced by the membrane association of +FWC, non-palmitoylated versions (Fig. 6*C*). It is possible that this affinity is insufficient to redirect a soluble protein but, in the context of an integral PM protein, is sufficient to enable lateral probing of the membrane surface (Fig. 8*C*). In some cases, this leads to transient interactions with specific partners, which in the case of Can1 and Alp1 are predicted to be integral membrane proteins (Fig. 8*D*). Possible interaction partners of Can1 might be found at the MCC/eisosome and relate to the patchy localization that has been observed previously (13). Eisosomes are static structures on the time scales of our measurements, but protein molecules may diffuse into and out of the MCC/eisosome with similar diffusion coefficients.

In conclusion, palmitoylated PM_{asseq} identified in the polytopic membrane proteins of the yeast plasma membrane represents a multipartite membrane association signal that has evolved toward multiple functions and may tune the location of proteins within specific membrane domains or binding of the proteins to specific partners and/or alter their function through self-regulatory mechanisms. Importantly, compared with other association signals in yeast, PM_{asseq} is relatively strong and has the potential to act as a delivery vehicle for the PM.

Experimental Procedures

Strains, Media, and Growth Conditions—All experiments were performed either in *S. cerevisiae* strains derived from BY4742 (48) or in *P. pastoris* strain KM71H (Invitrogen). See supplemental Table S3 for details.

S. cerevisiae strains were grown at 30 °C in synthetic complete dropout media, which contains 1× yeast nitrogen base without amino acids and 1× Kaiser amino acid dropout supplement (both from Formedium™, Norfolk, UK). The dropout supplements lacked histidine or uracil depending on the metabolic marker. 2% (w/v) raffinose, glucose, or glycerol was added as the carbon source to give SR, SD, or SG media, respectively. 2% (w/v) agar was added for plate cultures. *P. pastoris* strains were grown in YPD (2% (w/v) glucose, 1% (w/v) yeast extract, 2% (w/v) peptone) with 100 μg/ml Zeocin™ (Invitrogen).

In *S. cerevisiae*, reporter proteins were expressed either from the chromosome using their endogenous promoter and an mKate2 (49) tag or from low copy number plasmids using the *GAL1* promoter and a yeast enhanced GFP (50) tag (hereafter referred to as GFP). For expression from the *GAL1* promoter, strains were grown to midlog phase (A_{600} = 0.2–0.6) in SR medium and induced by the addition of 0.2% (w/v) galactose. In *P. pastoris*, proteins were expressed from episomal plasmids based on pBGP1 (51) using the constitutive *GAP* promoter and a GFP tag. Unless stated otherwise, all chemicals, reagents, and primers were purchased from Sigma-Aldrich. Restriction enzymes were purchased from New England Biolabs (Ipswich, MA).

Plasmid Construction—All plasmids were cloned first in *Escherichia coli* MC1061 and then isolated, confirmed by sequencing, and transformed into either *S. cerevisiae* or *P. pastoris* strains (supplemental Table S4). C terminus-coding sequences were amplified from BY4742 genomic DNA by polymerase chain reaction (PCR) and inserted into the target vectors using restriction digestion and ligation. Details of the primers and restriction sites used for each construct are given in supplemental Table S5. For N-terminal GFP fusions with or without a tcNLS, the termini were ligated into pACM021-GFP-tcNLS and pACM052-GFP, respectively. Variants of pDP001-GFP-Gap1C with C-terminal deletions were constructed by amplifying the plasmid using phosphorylated primers designed to bind directly upstream and downstream of the excluded sequence. The resulting PCR product was circularized via blunt end ligation.

The vector pFB008 was constructed using uracil excision-based cloning (52). The pUG72 plasmid was amplified in two fragments using primer pairs Pr50/53 and Pr51/52, respectively. The mKate2 sequence was amplified from a synthetically engineered plasmid (GeneArt, Regensburg, Germany) using primer pair Pr54/55. The fragments were treated with DNA glycosidase and DNA glycosylase-lyase endo VIII (commercially available as USER) following the manufacturer's instructions (New England Biolabs).

To achieve constitutive cytosolic expression in *P. pastoris*, the α-factor signal sequence was removed from pBGP1 (51) to create pBGP1na. Primer pair Pr70/71 was used to amplify the entire plasmid excluding the signal sequence. The resulting DNA fragment was circularized by uracil excision cloning as described above. The coding sequences for GFP-Gap1C, -Hip1C, and -Bap2C were amplified from pDP001, pDP008, and pDP0012, respectively, using primer pair Pr72/73. The vector pBGP1na was amplified using primer pair Pr74/75, and the coding sequences were inserted by uracil excision cloning.

FWS mutants of GFP-Bap2C and GFP-Hip1C were generated by PCR amplification from pDP008 and pDP012 using primer pairs Pr76/35 and Pr76/36. The DNA fragments were then restriction digested and ligated into pACM021-GFP and pBGP1na using BamHI/XhoI and NdeI/XhoI, respectively.

Strain Engineering—For the construction of C-terminal fusion proteins on the chromosome (supplemental Table S3), we made use of the mKate2-*URA3* cassette from pFB008. For C-terminal tagging of *CAN1*, *LYP1*, *GAP1*, and *TAT2* with or without the sequence coding for the last 10 amino acids, the cassette was amplified using primer pairs Pr58/55-56, Pr61/59-60, Pr64/62-63, and Pr67/65-66, respectively. The PCR products were transformed into *S. cerevisiae* BY4742 and selected for growth on uracil dropout medium. The genomic integration was verified by PCR and sequencing of the locus.

Fluorescence Imaging and FRAP Measurements—Fluorescence imaging and FRAP measurements were performed on an LSM 710 commercial scanning confocal microscope (Carl Zeiss MicroImaging, Jena, Germany) equipped with a C-Apochromat 40×/1.2 numerical aperture objective, a blue argon ion laser (488 nm) and a red helium-neon laser (633 nm). Cells were immobilized with hydrogel (Biomade, Groningen, Netherlands) between a glass slide and coverslip. Images were obtained with the focal plane positioned at the midsection of the cells.

For FRAP measurements, a region with a diameter of ~1 μm was photobleached using a short (26-μs) focused high power light pulse. The sample was imaged once immediately before the photobleaching and afterward for a period of 2400 or 20 s with frame rates of 20, 1, or 0.25 s for polytopic plasma membrane proteins, palmitoylated C termini, or C termini without lipid anchor, respectively. During the experiment, the sample was heated to 30 °C using a PeCon climate chamber. Data analysis was carried out in ImageJ (53, 54). Images were corrected for *xy* drift using cross-correlation fitting. Photobleaching due to imaging was corrected by fitting the fluorescence intensity of the entire image over time to a single exponential decay. The bleaching area was selected, and the recovery was fitted with Equation 1 to find the half-time of recovery.

$$f(t) = A\left(1 - e^{-\frac{\ln(2)}{\tau_{1/2}}t}\right) \quad \text{(Eq. 1)}$$

where A is normalized recovery, $\tau_{1/2}$ is half-time of recovery, and t is time in seconds.

The diffusion coefficient was estimated according to Equation 2 derived from Axelrod *et al.* (53).

$$D = \gamma \frac{w^2}{4t_{1/2}} \quad \text{(Eq. 2)}$$

where D is the diffusion coefficient, w is the radius of the bleaching spot, $t_{1/2}$ is the half-time of recovery, and γ is a correction factor (0.88 for circular beams). The radius of the bleaching spot was 1.0 ± 0.1 μm as determined previously (55, 56).

For strains carrying chromosomal mKate2 fusions, imaging was carried out on a fully automated home-built microscope. A wide field single molecule fluorescence microscope was constructed by coupling high power laser excitation into a commercially available inverted fluorescence microscope body (IX-81, Olympus, Tokyo, Japan) equipped with a 1.49 numerical aperture 100× objective and a 512 × 512 pixel electron-multiplying charge-coupled device camera (C9100-13, Hamamatsu). Excitation light was provided by continuous wave optically pumped semidiode lasers (Sapphire LP, Coherent Inc.) of wavelength 568 nm (200-milliwatt maximum output). For imaging mKate2 fusions, we used 568 nm excitation light and collected light emitted between 610 and 680 nm (ET 645/75m filter, Chroma).

Growth Assay—Strains expressing an mKate2 fusion with or without deletion of the last 10 C-terminal amino acids were precultured in SD over 48 h to midlog phase (A_{600} = 0.2–0.6) by three subsequent dilutions approximately every 12 h. Cells were washed and adjusted to an A_{600} of 0.2. Serial 10-fold dilutions were prepared, and 4 μl of each was spotted on SD or SG agar plates. Plates were imaged after a period of 3 or 4 days of growth at 30 °C (SD and SG, respectively).

Analysis of Palmitoylation by SDS-PAGE—Midlog phase cells were washed and resuspended to an A_{600} of 200 in 50 mM Tris-HCl (pH 7.6), 5 mM EDTA, 10% glycerol, Roche Applied Science cOmplete protease inhibitor mixture EDTA-free. Acid washed glass beads (500-μm diameter) were added in a 1:1 ratio with the cells. Cells were disrupted in a TissueLyser LT (Qiagen) at 30 Hz for 7 min. Unbroken cells were removed by centrifugation at 22,000 × *g* in a desktop centrifuge for 5 s at 4 °C. The supernatant was removed, and a total membrane fraction was collected by centrifugation in a desktop ultracentrifuge at 120,000 × *g* for 1 h at 4 °C. The total sample, supernatant, and membrane fractions were prepared for SDS-PAGE by addition of a 5× Laemmli buffer (250 mM Tris (pH 6.0), 50% (v/v) glycerol, 0.005% (w/v) bromphenol blue, 1% (w/v) SDS). For reducing conditions, 50 mM DTT was added and incubated prior to SDS-PAGE. Samples with and without DTT were separated by 15% SDS-PAGE at 240 V for 3 h at 20 °C. For whole cell extracts without DTT, samples were separated on a 20-cm-long 21% SDS-polyacrylamide gel run at 120 V for 48 h at 4 °C. In-gel fluorescence images were collected using a Fujifilm FLA-3000.

Circular Dichroism—Peptides corresponding to the last 31 residues of Gap1 with or without the truncations ΔEEK, ΔPRWYR, and ΔFWC were purchased from GeneCust (Luxembourg, Belgium). Samples used for CD measurements were 0.2 mg/ml in 1.67 mM sodium phosphate (equal molarity dibasic and tribasic), 0.33 mM DTT, 0–30% 2,2,2-trifluoroethanol. CD spectra were recorded on a Jasco J-715 spectropolarimeter using a bandwidth of 2 nm and a scanning speed of 50 nm/min. The spectra shown are an average of 15 scans. Measurements were carried out at 20 °C in a 0.1-cm-path length quartz cuvette.

Bioinformatics Analysis—UniProtKB (57) was searched for Swiss-Prot (manually annotated and reviewed) entries assigned to the three superfamilies (APC, AAPTII, and MFS) that contain the majority of the amino acid transporters in *S. cerevisiae*. The amino acid vacuolar transport family is classified by the Transporter Classification Database (58) as belonging to the amino acid/auxin permease family; however, this terminology is not maintained in UniProtKB. UniRef (59) was used to collapse each group of proteins into sequence clusters with 90% identity. The reference sequences for each UniRef90 cluster were then analyzed using TOPCONS-single (23) to determine the lengths of the N and C termini.

For further sequence analysis, we considered only core members of the AAP family from *S. cerevisiae* (1). These are the same 18 proteins classified by Saier (2) as belonging to the yeast amino acid transporter family. Multiple sequence alignments were generated using MAFFT (60) and visualized in Jalview (61). Secondary structure predictions were made using JPred4 (62), and NetTurnP (63). Helical wheel projections were generated manually. Hydrophobic moment values were calculated using the method of Eisenberg *et al.* (64) with the EMBOSS program hmoment using an angle of rotation of 100° and a window covering the entire predicted helix.

To explore conservation in other yeast species, UniRef (59) was used to collect sequences with >50% identity to *S. cerevisiae* FWC-containing AAPs and <90% identity to each other (198 proteins). Topology was predicted in batch mode by TOPCONS-single (23), and any proteins not predicted to have 12 transmembrane segments were run individually through TOPCONS (65) to be checked. In all cases, this resulted in a prediction of 12 transmembrane segments. The predicted C-terminal sequences were aligned using the MAFFT (60) online server, and the resulting alignment was manually trimmed to remove sequences causing gaps (180 proteins).

Author Contributions—D. P.-C., F. B., and B. P. designed research. D. P.-C., F. B., S. J. R., and F. M. performed research. D. P.-C., F. B., S. J. R., and B. P. analyzed data. D. P.-C., F. B., and B. P. wrote the paper.

Acknowledgment—We are grateful to Joury van 't Klooster for support with the CD measurements.

References

1. Ljungdahl, P. O., and Daignan-Fornier, B. (2012) Regulation of amino acid, nucleotide, and phosphate metabolism in *Saccharomyces cerevisiae*. *Genetics* **190,** 885–929
2. Saier, M. H. (2000) Families of transmembrane transporters selective for amino acids and their derivatives. *Microbiology* **146,** 1775–1795
3. Donaton, M. C., Holsbeeks, I., Lagatie, O., Van Zeebroeck, G., Crauwels, M., Winderickx, J., and Thevelein, J. M. (2003) The Gap1 general amino acid permease acts as an amino acid sensor for activation of protein kinase A targets in the yeast *Saccharomyces cerevisiae*. *Mol. Microbiol.* **50,** 911–929
4. Giots, F., Donaton, M. C., and Thevelein, J. M. (2003) Inorganic phosphate is sensed by specific phosphate carriers and acts in concert with glucose as a nutrient signal for activation of the protein kinase A pathway in the yeast *Saccharomyces cerevisiae*. *Mol. Microbiol.* **47,** 1163–1181
5. Van Nuland, A., Vandormael, P., Donaton, M., Alenquer, M., Lourenço, A., Quintino, E., Versele, M., and Thevelein, J. M. (2006) Ammonium permease-based sensing mechanism for rapid ammonium activation of the protein kinase A pathway in yeast. *Mol. Microbiol.* **59,** 1485–1505
6. Didion, T., Regenberg, B., Jørgensen, M. U., Kielland-Brandt, M. C., and Andersen, H. A. (1998) The permease homologue Ssy1p controls the expression of amino acid and peptide transporter genes in *Saccharomyces cerevisiae*. *Mol. Microbiol.* **27,** 643–650
7. Klasson, H., Fink, G. R., and Ljungdahl, P. O. (1999) Ssy1p and Ptr3p are plasma membrane components of a yeast system that senses extracellular amino acids. *Mol. Cell. Biol.* **19,** 5405–5416
8. Kralt, A., Carretta, M., Mari, M., Reggiori, F., Steen, A., Poolman, B., and Veenhoff, L. M. (2015) Intrinsically disordered linker and plasma membrane-binding motif sort Ist2 and Ssy1 to junctions. *Traffic* **16,** 135–147
9. Hinnebusch, A. G., and Natarajan, K. (2002) Gcn4p, a master regulator of gene expression, is controlled at multiple levels by diverse signals of starvation and stress. *Eukaryot. Cell.* **1,** 22–32
10. Natarajan, K., Meyer, M. R., Jackson, B. M., Slade, D., Roberts, C., Hinnebusch, A. G., and Marton, M. J. (2001) Transcriptional profiling shows that Gcn4p is a master regulator of gene expression during amino acid starvation in yeast. *Mol. Cell. Biol.* **21,** 4347–4368
11. Lin, C. H., MacGurn, J. A., Chu, T., Stefan, C. J., and Emr, S. D. (2008) Arrestin-related ubiquitin-ligase adaptors regulate endocytosis and protein turnover at the cell surface. *Cell* **135,** 714–725
12. Cooper, T. G. (1982) Nitrogen metabolism in *Saccharomyces cerevisiae*, in *The Molecular Biology of the Yeast Saccharomyces: Metabolism and Gene Expression*, Cold Spring Harbor Monograph Archive Vol. 11B, pp. 39–99, Cold Spring Harbor Laboratory Press, Cold Spring Harbor, NY
13. Malinska, K., Malinsky, J., Opekarova, M., and Tanner, W. (2004) Distribution of Can1p into stable domains reflects lateral protein segregation within the plasma membrane of living *S. cerevisiae* cells. *J. Cell Sci.* **117,** 6031–6041
14. Vivero-Pol, L., George, N., Krumm, H., Johnsson, K., and Johnsson, N. (2005) Multicolor imaging of cell surface proteins. *J. Am. Chem. Soc.* **127,** 12770–12771
15. Spira, F., Mueller, N. S., Beck, G., von Olshausen, P., Beig, J., and Wedlich-Söldner, R. (2012) Patchwork organization of the yeast plasma membrane into numerous coexisting domains. *Nat. Cell Biol.* **14,** 640–648
16. Blobel, G. (1980) Regulation of intracellular protein traffic. *Harvey Lect.* **76,** 125–147
17. Dingwall, C., Sharnick, S. V., and Laskey, R. A. (1982) A polypeptide domain that specifies migration of nucleoplasmin into the nucleus. *Cell.* **30,** 449–458
18. Dingwall, C., and Laskey, R. A. (1991) Nuclear targeting sequences—a consensus? *Trends Biochem. Sci.* **16,** 478–481
19. Gao, M., and Kaiser, C. A. (2006) A conserved GTPase-containing complex is required for intracellular sorting of the general amino-acid permease in yeast. *Nat. Cell Biol.* **8,** 657–667
20. Cornell, R. B., and Taneva, S. G. (2006) Amphipathic helices as mediators of the membrane interaction of amphitropic proteins, and as modulators of bilayer physical properties. *Curr. Protein Pept. Sci.* **7,** 539–552
21. Malínská, K., Malínský, J., Opekarová, M., and Tanner, W. (2003) Visualization of protein compartmentation within the plasma membrane of living yeast cells. *Mol. Biol. Cell.* **14,** 4427–4436
22. Roth, A. F., Wan, J., Bailey, A. O., Sun, B., Kuchar, J. A., Green, W. N., Phinney, B. S., Yates, J. R., 3rd, and Davis, N. G. (2006) Global analysis of protein palmitoylation in yeast. *Cell.* **125,** 1003–1013
23. Hennerdal, A., and Elofsson, A. (2011) Rapid membrane protein topology prediction. *Bioinformatics* **27,** 1322–1323
24. Gatto, G. J., Jr., and Berg, J. M. (2003) Nonrandom tripeptide sequence distributions at protein carboxyl termini. *Genome Res.* **13,** 617–623
25. Hein, C., and André, B. (1997) A C-terminal di-leucine motif and nearby sequences are required for NH_4^+-induced inactivation and degradation of the general amino acid permease, Gap1p, of *Saccharomyces cerevisiae*. *Mol. Microbiol.* **24,** 607–616
26. Greenfield, N. J. (2006) Using circular dichroism spectra to estimate protein secondary structure. *Nat. Protoc.* **1,** 2876–2890
27. Sönnichsen, F. D., Van Eyk, J. E., Hodges, R. S., and Sykes, B. D. (1992) Effect of trifluoroethanol on protein secondary structure: an NMR and CD study using a synthetic actin peptide. *Biochemistry* **31,** 8790–8798
28. Omura, F., Kodama, Y., and Ashikari, T. (2001) The basal turnover of yeast branched-chain amino acid permease Bap2p requires its C-terminal tail. *FEMS Microbiol. Lett.* **194,** 207–214
29. Manford, A. G., Stefan, C. J., Yuan, H. L., Macgurn, J. A., and Emr, S. D. (2012) ER-to-plasma membrane tethering proteins regulate cell signaling and ER morphology. *Dev. Cell* **23,** 1129–1140
30. Maass, K., Fischer, M. A., Seiler, M., Temmerman, K., Nickel, W., and Seedorf, M. (2009) A signal comprising a basic cluster and an amphipathic α-helix interacts with lipids and is required for the transport of Ist2 to the yeast cortical ER. *J. Cell Sci.* **122,** 625–635
31. Jüschke, C., Wächter, A., Schwappach, B., and Seedorf, M. (2005) SEC18/NSF-independent, protein-sorting pathway from the yeast cortical ER to the plasma membrane. *J. Cell Biol.* **169,** 613–622
32. Celton-Morizur, S., Bordes, N., Fraisier, V., Tran, P. T., and Paoletti, A. (2004) C-terminal anchoring of mid1p to membranes stabilizes cytokinetic ring position in early mitosis in fission yeast. *Mol. Cell. Biol.* **24,** 10621–10635
33. Winters, M. J., Lamson, R. E., Nakanishi, H., Neiman, A. M., and Pryciak, P. M. (2005) A membrane binding domain in the ste5 scaffold synergizes with $G\beta\gamma$ binding to control localization and signaling in pheromone response. *Mol. Cell* **20,** 21–32
34. Meinema, A. C., Laba, J. K., Hapsari, R. A., Otten, R., Mulder, F. A., Kralt, A., van den Bogaart, G., Lusk, C. P., Poolman, B., and Veenhoff, L. M. (2011) Long unfolded linkers facilitate membrane protein import through the nuclear pore complex. *Science* **333,** 90–93
35. Linder, M. E., and Deschenes, R. J. (2003) New insights into the mechanisms of protein palmitoylation. *Biochemistry* **42,** 4311–4320
36. Springael, J. Y., and André, B. (1998) Nitrogen-regulated ubiquitination of the Gap1 permease of *Saccharomyces cerevisiae*. *Mol. Biol. Cell.* **9,** 1253–1263
37. Nishimura, N., and Balch, W. E. (1997) A di-acidic signal required for selective export from the endoplasmic reticulum. *Science* **277,** 556–558
38. Malkus, P., Jiang, F., and Schekman, R. (2002) Concentrative sorting of secretory cargo proteins into COPII-coated vesicles. *J. Cell Biol.* **159,** 915–921
39. Atwal, R. S., Xia, J., Pinchev, D., Taylor, J., Epand, R. M., and Truant, R. (2007) Huntingtin has a membrane association signal that can modulate huntingtin aggregation, nuclear entry and toxicity. *Hum. Mol. Genet.* **16,** 2600–2615
40. Loewen, C. J., Gaspar, M. L., Jesch, S. A., Delon, C., Ktistakis, N. T., Henry, S. A., and Levine, T. P. (2004) Phospholipid metabolism regulated by a

transcription factor sensing phosphatidic acid. *Science* **304,** 1644–1647
41. Neiman, A. M., Katz, L., and Brennwald, P. J. (2000) Identification of domains required for developmentally regulated SNARE function in *Saccharomyces cerevisiae*. *Genetics* **155,** 1643–1655
42. Pryciak, P. M., and Huntress, F. A. (1998) Membrane recruitment of the kinase cascade scaffold protein Ste5 by the G$\beta\gamma$ complex underlies activation of the yeast pheromone response pathway. *Genes Dev.* **12,** 2684–2697
43. Drogen, F., O'Rourke, S. M., Stucke, V. M., Jaquenoud, M., Neiman, A. M., and Peter, M. (2000) Phosphorylation of the MEKK Ste11p by the PAK-like kinase Ste20p is required for MAP kinase signaling *in vivo*. *Curr. Biol.* **10,** 630–639
44. Endres, N. F., Das, R., Smith, A. W., Arkhipov, A., Kovacs, E., Huang, Y., Pelton, J. G., Shan, Y., Shaw, D. E., Wemmer, D. E., Groves, J. T., and Kuriyan, J. (2013) Conformational coupling across the plasma membrane in activation of the EGF receptor. *Cell.* **152,** 543–556
45. Smets, B., Ghillebert, R., De Snijder, P., Binda, M., Swinnen, E., De Virgilio, C., and Winderickx, J. (2010) Life in the midst of scarcity: adaptations to nutrient availability in *Saccharomyces cerevisiae*. *Curr. Genet.* **56,** 1–32
46. Cornell, R. B., and Northwood, I. C. (2000) Regulation of CTP:phosphocholine cytidylyltransferase by amphitropism and relocalization. *Trends Biochem. Sci.* **25,** 441–447
47. Giaever, G., Chu, A. M., Ni, L., Connelly, C., Riles, L., Véronneau, S., Dow, S., Lucau-Danila, A., Anderson, K., André, B., Arkin, A. P., Astromoff, A., El-Bakkoury, M., Bangham, R., Benito, R., *et al.* (2002) Functional profiling of the *Saccharomyces cerevisiae* genome. *Nature* **418,** 387–391
48. Brachmann, C. B., Davies, A., Cost, G. J., Caputo, E., Li, J., Hieter, P., and Boeke, J. D. (1998) Designer deletion strains derived from *Saccharomyces cerevisiae* S288C: a useful set of strains and plasmids for PCR-mediated gene disruption and other applications. *Yeast* **14,** 115–132
49. Piatkevich, K. D., Hulit, J., Subach, O. M., Wu, B., Abdulla, A., Segall, J. E., and Verkhusha, V. V. (2010) Monomeric red fluorescent proteins with a large Stokes shift. *Proc. Natl. Acad. Sci. U.S.A.* **107,** 5369–5374
50. Cormack, B. P., Bertram, G., Egerton, M., Gow, N. A., Falkow, S., and Brown, A. J. (1997) Yeast-enhanced green fluorescent protein (yEGFP): a reporter of gene expression in *Candida albicans*. *Microbiology* **143,** 303–311
51. Lee, C. C., Williams, T. G., Wong, D. W., and Robertson, G. H. (2005) An episomal expression vector for screening mutant gene libraries in *Pichia pastoris*. *Plasmid.* **54,** 80–85
52. Bitinaite, J., and Nichols, N. M. (2009) DNA cloning and engineering by uracil excision. *Curr. Protoc. Mol. Biol.* **Chapter 3,** Unit 3.21
53. Axelrod, D., Koppel, D. E., Schlessinger, J., Elson, E., and Webb, W. W. (1976) Mobility measurement by analysis of fluorescence photobleaching recovery kinetics. *Biophys. J.* **16,** 1055–1069
54. Schneider, C. A., Rasband, W. S., and Eliceiri, K. W. (2012) NIH Image to ImageJ: 25 years of image analysis. *Nat. Methods* **9,** 671–675
55. Meinema, A. C., Poolman, B., and Veenhoff, L. M. (2013) Quantitative analysis of membrane protein transport across the nuclear pore complex. *Traffic* **14,** 487–501
56. Phillips, R., Kondev, J., Theriot, J., and Garcia, H. G. (2013) *Physical Biology of the Cell*, p. 525, Garland Science, New York
57. Magrane, M., and UniProt Consortium (2011) UniProt Knowledgebase: a hub of integrated protein data. *Database* **2011,** bar009
58. Saier, M. H. (2000) A functional-phylogenetic classification system for transmembrane solute transporters. *Microbiol. Mol. Biol. Rev.* **64,** 354–411
59. Suzek B. E., Wang Y., Huang H., McGarvey P. B., Wu C. H., and UniProt Consortium (2015) UniRef clusters: a comprehensive and scalable alternative for improving sequence similarity searches. *Bioinformatics* **31,** 926–932
60. Katoh, K., and Standley, D. M. (2013) MAFFT multiple sequence alignment software version 7: improvements in performance and usability. *Mol. Biol. Evol.* **30,** 772–780
61. Waterhouse, A. M., Procter, J. B., Martin, D. M., Clamp, M., and Barton, G. J. (2009) Jalview Version 2—a multiple sequence alignment editor and analysis workbench. *Bioinformatics* **25,** 1189–1191
62. Drozdetskiy, A., Cole, C., Procter, J., and Barton, G. J. (2015) JPred4: a protein secondary structure prediction server. *Nucleic Acids Res.* **43,** W389–W394
63. Petersen, B., Lundegaard, C., and Petersen, T. N. (2010) NetTurnP—neural network prediction of β-turns by use of evolutionary information and predicted protein sequence features. *PLoS One* **5,** e15079
64. Eisenberg, D., Weiss, R. M., and Terwilliger, T. C. (1984) The hydrophobic moment detects periodicity in protein hydrophobicity. *Proc. Natl. Acad. Sci. U.S.A.* **81,** 140–144
65. Bernsel, A., Viklund, H., Hennerdal, A., and Elofsson, A. (2009) TOPCONS: consensus prediction of membrane protein topology. *Nucleic Acids Res.* **37,** W465–W468
66. Crooks, G. E., Hon, G., Chandonia, J.-M., and Brenner, S. E. (2004) WebLogo: a sequence logo generator. *Genome Res.* **14,** 1188–1190